Comparisons on Performances in MIMO Systems under Different Propagation Environments

Jun Sun and Hongbo Zhu

Institute of Communication Technology,
Key Laboratory of Wireless Communications, Jiangsu Province,
Nanjing University of Posts and telecommunications,
Nanjing, JiangSu, 210003
freyjajune@163.com

Abstract. [1] The purpose of this paper is to study how the different propagation environments as well as antenna configurations impact on the performances of space-time block coded (STBC) MIMO systems. Based on the geometrical differences such as one-ring model and elliptical model with different distributions of scatters, the comparisons on system performances are presented here. The impacts of the mean spread of the angle of arrival (AOA), the width of AOA and the antenna array configuration are included in the discussion. According to the geometrical models, analytical expressions of spatial cross-correlation functions are derived. The results show that the power efficiency and spectral efficiency are influenced differently by the antenna array configuration. So, thresholds of these impacts are found finally. Besides, a closed-form expression of a new upper bound of the ergodic capacity for STBC MIMO systems is also given here.

1 Introduction

In recent decade years, the research on the performances of the MIMO system has received much attention for its advantages inherently, especially the space time block coded (STBC) [1]-[3] MIMO systems, which integrate the techniques of spatial diversity and channel codings. It is well known that, the communication quality can be worse when the fading are correlated. The authors in [4] provided an upper bound of the capacity including the number of transmit and receive antennas, achieved by orthogonal STBC over Rayleigh channels with adaptive transmission and channel estimation errors. The error probability of STBC has been approximated first by Gozali *et.al.* in [5] in the case of correlated Rayleigh fading, then by Femenias in [6], in the case of Nakagami fading channels.

It shows [7] that the performances of MIMO systems depend strongly on the channel characteristics, especially the spatial correlations. Meanwhile, the spatial

[1] This paper is supported by National 973 project[2007CB310600]; NNSF project[60432040]; NNSF project[60572024]; China Education Ministry Doctor Foundation[20050293003]; China Poster Doctor Foundation[20080441067]; Province Poster Doctor Foundation[0802017B], 863[2009AA011300].

K. Sithamparanathan (Ed.): Psats 2009, LNICST 15, pp. 111–121, 2009.

correlation is determined by the physical environment, such as the antenna configuration and the scattering distribution. An overview of MIMO channel models can be found in [8]. The capacity of narrowband flat fading MIMO channels can be found in [9]-[10].

In this paper, we first analysis the spatial cross-correlation functions of two typical MIMO channels, the one-ring model and the elliptical model. Then, we study the impacts of the spatial cross-correlation on the ergodic capacity and BER performance in STBC MIMO systems. Meanwhile, we deduce a new upper bound of ergodic capacity for any practical application from the moment generating function (MGF) point of view.

2 System Model

The system model here is the same as that in [4]. There are n_T antenna elements at the transmitter and n_R antenna elements at the receiver. The maximum diversity gain is $K = n_T n_R$. The channel coherent time is T symbols and each symbol is transmitted with an average power E_s. The input-output relationship can be expressed as:

$$Y = Hg + V \tag{1}$$

Where, Y is an $n_R \times T$ received signal matrix, g is an $n_T \times T$ transmitted symbols matrix and V is an $n_R \times T$ additive noise matrix whose elements are the samples of i.i.d. complex circular Gaussian random variables with zero-mean and the average power $\sigma^2 = N_0$. The element in $H = [h_{ij}]_{i,j=1}^{n_R,n_T}$ is a complex gain of one realization of the random variable $h_{ij}, i = 1, \cdots, n_R, j = 1, \cdots, n_T$. The function $h_{ij}(t)$ is a typical impulse response of a narrowband linear, quasi-stationary, multipath fading environment in MIMO systems. The effective output of CSNR at sample point η at the receiver in STBC MIMO systems is given by

$$\gamma = \frac{\overline{\gamma}}{n_T R_c} \left\| H_\eta \right\|_F^2 \tag{2}$$

Where, $\bar{\gamma} = E_s/N_0$ is the average CSNR per receive antenna and R_c is the code rate of STBC which is defined as the rate of the input signal symbols R and T. Generally, $R_c \leq 1$ and here $R_c = 1$. The factor $\left\| H_\eta \right\|_F$ is the Frobenius form defined by

$$\left\| H_\eta \right\|_F = \sqrt{\sum\nolimits_{i=1}^{n_R} \sum\nolimits_{j=1}^{n_T} \left| h_{i,j} \right|^2} = \sqrt{trace(H_\eta H_\eta^H)} \tag{3}$$

When $p_{\zeta_\eta}(\zeta_\eta)$ is the PDF of the variable $\zeta_\eta = \left\| H_\eta \right\|_F^2$, the MGF of ζ_η can be defined as [11]

$$M_{\zeta_\eta}(s) = E\{e^{-s\zeta_\eta}\} = \int_{-\infty}^{\infty} e^{-s\zeta_\eta} p_{\zeta_\eta}(\zeta_\eta) d\zeta_\eta \tag{4}$$

According to Luo *et al.* in [12], (4) can be written as

$$M_{\zeta_\eta}(s) = \det(I_{n_R n_T} + s\frac{\Omega}{m}\Lambda)^{-m} \tag{5}$$

Where, $I_{n_R n_T}$ is the $n_R n_T \times n_R n_T$ identity matrix and $\Lambda = [\rho_{\mathrm{ij,i'j'}}]$ is a positive define covariance matrix. The spatial cross correlation between $h_{ij,\eta}$ and $h_{i'j',\eta}$ at the η block can be expressed as in [8]

$$\begin{aligned}\rho_{\mathrm{ij,i'j'}} &= \frac{E\{h_{ij,\eta}, h_{\mathrm{i'j'},\eta}\}}{\sqrt{\Omega_{\mathrm{ij}}\Omega_{\mathrm{i'j'}}}} \\ &= \int_{-\pi}^{\pi} \exp[-j\tfrac{2\pi}{\lambda}\Xi_{ij,\mathrm{i'j'},\eta}(\phi^{MT})] f_{\phi^{MT}}(\phi^{MT}) d\phi^{MT}\end{aligned} \tag{6}$$

Where,

$$\Omega_{ij} = E\{|h_{ij,\eta}|^2\} = \sum_{q=1}^{m} \sum_{p=1}^{I_{q,ij,\eta}} E\{|g_{pq,\eta}|^2\} = \Omega \tag{7}$$

And, $\Xi_{ij,\mathrm{i'j'},\eta}(\phi^{MT})$ is the distance parameter defined in [13].

3 Channel Models

The spatial correlation coefficient in (6) changes as geometrical distribution of propagation varying. According to the rectangle method of the numerical analysis, (6) can be written as

$$\rho_{ij,i'j'} \approx \Delta_\phi \left(\sum_{l=1}^{L} \exp[-j\frac{2\pi}{\lambda}\Xi_{ij,i'j',\eta}(\phi_l^{MT})] f_{\phi_l^{MT}}(\phi_l^{MT})\right) \tag{8}$$

Where, $\phi_l^{MT} = -\pi + \Delta_\phi \cdot l$, and $\Delta_\phi = 2\pi/L$ and L is the number of the samples in range $[-\pi, \pi]$. Here, we employ a 2×2 MIMO system and assume that the antenna configuration satisfies the following assumptions. The space of the transmit (receive) antenna array is d_{BS} (d_{MT}). The angle between the horizontal line and the transmit (receiver) antenna array is α_{BS} (α_{MT}).

The value of (8) depends on $\Xi_{ij,i'j',\eta}(\phi_l^{MT})$ which is determined by different geometrical models. Consider a one-ring model in [6] which is assumed that BS is elevated and not obstructed by local scatters, while MT is surrounded by an infinite number of local scatters laying on a ring. Assume that the radius of the ring is R and the distance between the BS and the MT is D. The point on the ring of the *pth* scatter in the *qth* group determined by ϕ^{MT} is S_{pq}. The distance from the center of the transmit antenna array to the point S_{pq} is $\xi_\eta^{BS}(\phi^{MT})$ which is a function of ϕ^{MT}. Similarly, the distance from the center of the receive antenna array to the point S_{pq} is R. The angle between the horizonal line and ξ_η^{BS} (or R) is ϕ_η^{BS} (or ϕ^{MT}). There are

$$\phi_\eta^{BS} = \arctan\left(\frac{R \cdot \sin(\phi^{MT})}{D - R \cdot \cos(\phi^{MT})}\right) \tag{9}$$

and

$$\xi_\eta^{BS} = \sqrt{R^2 + D^2 - 2 \cdot R \cdot D \cdot \cos(\phi^{MT})} \tag{10}$$

When the scatters located at MT and BS as an elliptical, that is the model in [14] which has the same antenna configuration but different geometrical distribution.

The quantity R in one-ring model is replaced by the eccentricity parameter $\nu = 2a/D$ in elliptical model [14] . The parameter a presents half length of the major axis of the ellipse and D here is explained as the distance between the focal points. Then, the distances parameter can be calculated with the following changes

$$\phi_{\eta}^{BS} = \begin{cases} f(\phi^{MT}), 0 < \phi^{MT} \leq \phi^{\nu} \\ f(\phi^{MT}) + \pi, \phi^{\nu} < \phi^{MT} \leq 2\pi - \phi^{\nu} \\ f(\phi^{MT}) + 2\pi, 2\pi - \phi^{\nu} < \phi^{MT} \leq 2\pi \end{cases} \tag{11}$$

Where,

$$f(\phi^{MT}) = \arctan(\frac{(\nu^2 - 1)\sin(\phi^{MT})}{2\nu + (\nu^2 + 1)\cos(\phi^{MT})}) \tag{12}$$

and

$$\phi^{\nu} = \pi - \arctan(\frac{\nu^2 - 1}{2\nu}) \tag{13}$$

For simplicity's sake, we omit the sample index η in the following sections.

4 System Performances

The ergodic capacity of correlated Rayleigh STBC MIMO channels can be found in [15]. As shown in [6], the MGF $M_{\zeta}(s)$ of $\|H\|_F^2$ can be expressed as

$$M_{\zeta}(s) = \prod_{n=1}^{N} \frac{1}{(1 + s\aleph_n)^{m\alpha_n}} \tag{14}$$

where $\aleph_n = (\Omega/m)\lambda_n$ and $\{\lambda_n\}$ is the set of N distinct eigenvalues of Λ. The parameter α_n satisfies $\sum_{n=1}^{N} \alpha_n = n_R n_T$. Here, we suppose the channel parameters with $m = 1, \Omega = 1$. In [15], the authors gave the ergodic capacity in nats per seconds per hertz (nats/s/Hz). Now, we deduce an upper bound on the achievable capacity for any practical application from the MGF point of view. Apply Jensen's inequality, the ergodic capacity can be written as

$$\begin{aligned} C &\leq R_c \cdot \log(1 + E\{\tfrac{\overline{\gamma}}{R_c \cdot n_T} \|H\|_F^2\}) \\ &= R_c \cdot \log(1 + \tfrac{\overline{\gamma}}{R_c \cdot n_T} E[\|H\|_F^2]) \end{aligned} \tag{15}$$

Starting with the relationship between MGF and moment functions as following,

$$E[x^n] = \frac{d^n M_x(t)}{dt^n} \mid_{t=0} \tag{16}$$

where x is a random variable, the mean of $\|H\|_F^2$ can be calculated by

$$E[\|H\|_F^2] = \frac{dM_{\zeta}(s)}{ds} \mid_{s=0} \tag{17}$$

So, the mean is

$$E[\|H\|_F^2] = \sum\nolimits_{n=1}^{N} \lambda_n \tag{18}$$

Finally, the up bound of ergodic capacity is

$$C_{up} = R_c \cdot \log(1 + \frac{\overline{\gamma}}{R_c \cdot n_T} \sum\nolimits_{n=1}^{N} \lambda_n) \tag{19}$$

Besides, the analytical expressions of the BER performance for both integral and non-integral Nakagami-m fading parameters under MPSK and MQAM modulations can be found in [6]. The average BER of a linear STBC using MPSK modulation is rewritten here for the purpose of the analysis as a representation.

$$\begin{aligned} P_b(E) = \frac{2}{\pi \max(\log_2(M),2)} \sum_{i=1}^{\max(\frac{M}{4},1)} \\ \times \int_0^{\frac{\pi}{2}} M_\varsigma(\frac{\overline{\gamma}}{n_T} \frac{\sin^2(2i-1)\frac{\pi}{M}}{\sin^2\theta}) d\theta \end{aligned} \tag{20}$$

5 Numerical Analysis

In this section, first a series of numerical examples are presented to illustrate the influences of the antenna configuration and the propagation conditions on the spatial correlation coefficients. Then, we discuss the impacts of the eigenvalues of the channel covariance matrixes on the ergodic capacity and BER performance. Here, a 2×2 STBC MIMO system is employed. The code rate R_c, the average fading power Ω are both equal to one. The angle α_{BS} is $\pi/4$ and the angle α_{MT} is $3\pi/4$. The beamwidth Δ of $\arctan(R/D)$ is $\pi/16$ in the one-ring model. However, in the elliptical model, the eccentricity parameter $\nu = 1.5$.

BER performance. Fig.1 illustrates the influence of the antenna configuration for different channel models on the average BER performances of a $QPSK$ modulated 2×2 STBC MIMO system versus the average E_b/N_0. The capital "E" in the figure denotes an elliptical model and "O" denotes a one-ring model. A fixed spacing between the MT antenna elements $d_{12}^{MT}/\lambda = 0.3$ is assumed and $\alpha_{12}^{BS} = \pi/4, \alpha_{12}^{MT} = 3\pi/4$ for both models. Besides, the quantity Δ is $\pi/16$ for the one-ring model and ν is 1.5 for the elliptical model. The results have been found by evaluating (20) and relevant parameters. Firstly, for comparative purpose of different models, there is almost no difference of BER performance between the two models for $d_{12}^{BS} > 1$ at a fixed value of d_{12}^{MT}. When $d_{12}^{BS} \leq 1$, the BER performance under an elliptical channel model is better than that under a one-ring model. And the smaller the spacing is, the more obvious the difference is. This can be seen more obviously from Fig.2. Secondly, for the same model, the BER performance decreases as the separation between antenna elements decreases. This indicates the excellent accordance between the numerical results and the theoretical situation that the reliability descends because of the high space correlation of the antenna elements in MIMO systems.

For comparative purposes, we have also plotted the impact of the antenna configuration on the BER performance at MT with a fixed antenna spacing $d_{12}^{BS}/\lambda = 5$ in Fig.3. As it is readily apparent in the graph, the BER performance

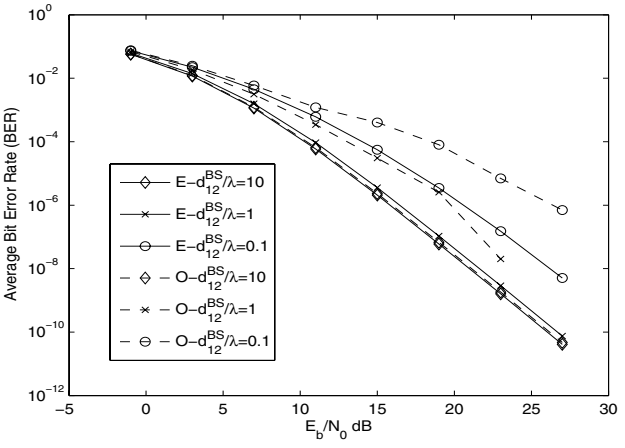

Fig. 1. The impact of the antenna configuration on the BER performance at BS I

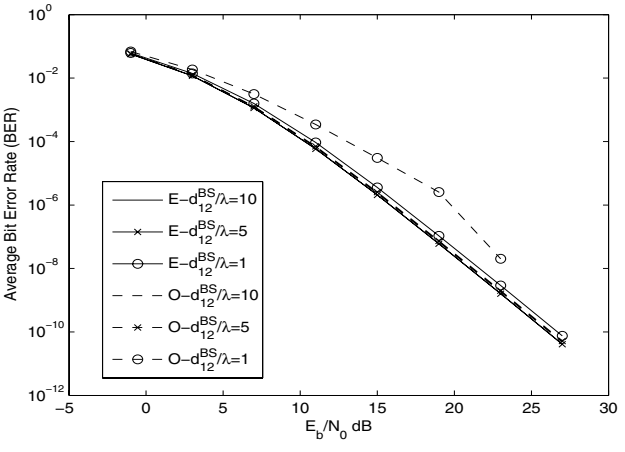

Fig. 2. The impact of the antenna configuration on the BER performance at BS II

is worse as the distance between the MT antenna elements decreases under the same channel model. And the impact is more remarkable under the one-ring model than that under the elliptical model. Similarly, there is also a bound for the affection like the situation at BS. It has almost the same BER performances for both the two models at $d_{12}^{MT} > 0.1$ with a fixed d_{12}^{BS} which is shown more clearly in Fig.4.

In order to interpret the impact of the width of AOA on BER performance, we draw the graph of BER with $d_{12}^{BS}/\lambda = 5, d_{12}^{MT}/\lambda = 0.3, M = 4$ under different value of κ in Fig.5. For the one-ring model case, the higher value of κ corresponding to the narrower width of AOA leads to higher BER performance. While for the elliptical model case, the situation is more complexity. First, the change is

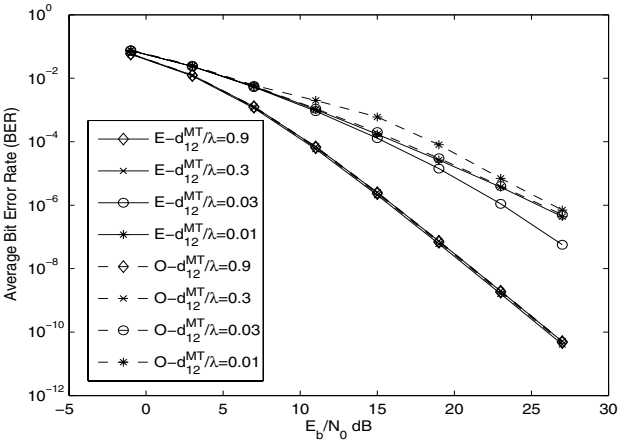

Fig. 3. The impact of the antenna configuration on the BER performance at MT I

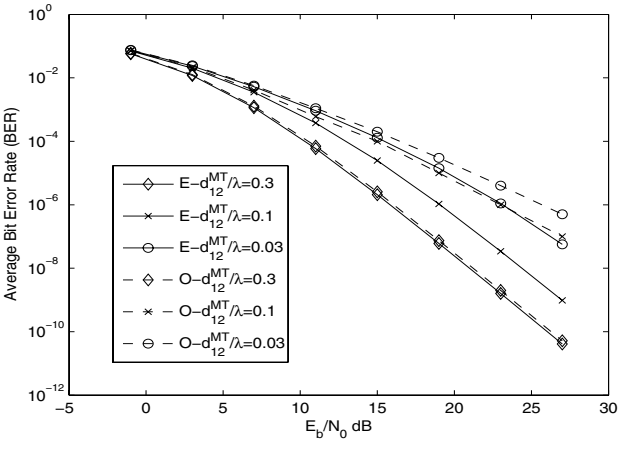

Fig. 4. The impact of the antenna configuration on the BER performance at MT II

not as remarkable as that at the one-ring case. Next, it seems that the narrower width of AOA does not bring the improvement of the BER performance.

Ergodic Capacity. In this section, we compare the ergodic capacity of the up bounds defined in [15] and (19) in Fig.6. The line denoted by 'Up Bound' is derived from [15] and the other two lines are derived from (19). It is clear that the capacity is almost independent on the antenna configuration and it is almost same under different models when the number of antenna elements and the rate of STBC are fixed. That is, the eigenvalues of different channel variance matrix has little impact on the bounds of ergodic capacity. Because the sum of them is

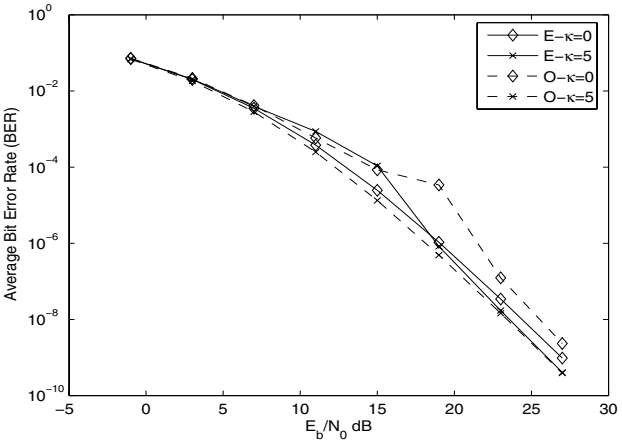

Fig. 5. BER performance comparison with $\kappa = 5$

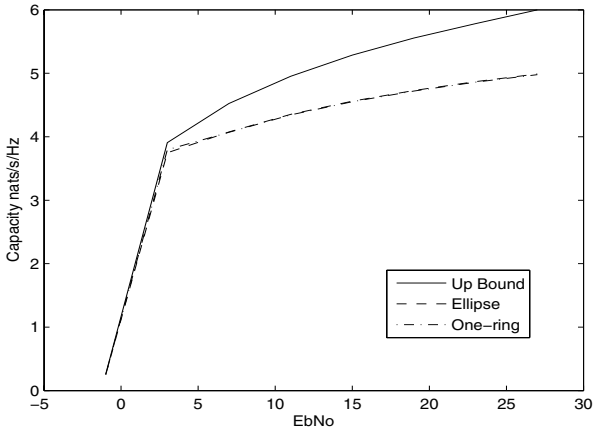

Fig. 6. The comparison of the ergodic capacity

always constant and equal to $n_T n_R$ according to (19). This result is similar to that in [15]. Besides, the new bound defined in (19) is upper than that in [15].

Efficiency versus Reliability. In order to interpret the influence of the communication conditions on the two important quality components, i.e., the efficiency and the reliability clearly, we show it in Fig.7. In this figure, the real line presents the up bound of the ergodic capacity derived from (19). We first show the impact of the M-PSK on the quality components in the same MIMO systems under different channel models. Then, the affect of the antenna configuration is discussed. Obviously, the systems using QPSK modulation have the

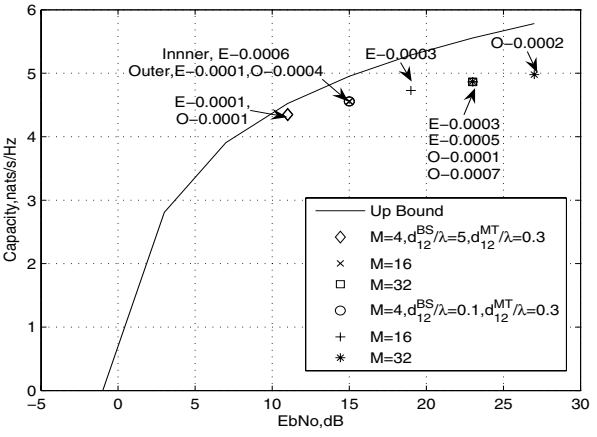

Fig. 7. Simulation Results

same efficiency and reliability under both the one-ring model and the elliptical model, which is denoted by the diamond dot in the figure. When the distance between the antenna elements at BS is shortened, the efficiency increases ($E - 0.0001, O - 0.0001$ and the corresponding capacity is 4.3517 and 4.3443, respectively.) for both channel models denoted by the circle dot in the figure, but the reliability under the one-ring model decreases ($E - 0.0001, O - 0.0004$). The corresponding capacity is 4.5604 and 4.5524, respectively. The same thing happens using other higher modulations, such as the multiplication sign and the crisscross dot in the graph derived from 16-PSK. Besides, for a certain model such as an elliptical model, it requires more bigger SNR in order to obtain the same BER performance if the system wants to use a higher modulation ($E - 0.0003$ denoted by crisscross dot and $E - 0.0003$ denoted by star dot). When the spacing between the antenna elements decreases, it also requires more SNR in order to keep the same efficiency and reliability quality for a system under one-ring models ($O - 0.0001$ denoted by square dot and $O - 0.0002$ denoted by star dot). It indicates again that the high space relation reduces the system performance.

6 Conclusion

From the analysis and the numerical results written above, we can make a conclusion in the following.

(i) The space correlation plays an important role in the analysis of the system performances. The impacts of an elliptical model are more remarkable than that of a one-ring model with the same antenna configuration;
(ii) For a certain geometrical propagation case, the antenna configuration affects system performances. In general, lower space correlation leads to better BER performance. However, there is almost no difference for the bounds of ergodic capacity among different geometical models;

(iii) For any geometrical model, there is a threshold for the space of the antenna elements, which determined whether the distribution of scatters or the propagation conditions affect BER performance. At BS, the threshold space is about one λ and it is about 0.1λ at MT;
(iv) When the distance is below the threshold, the impacts of the geometrical conditions are primary;
(v) Different κ influence the BER performance differently. For the one-ring model case, higher κ leads to higher BER performance. However, the situation is more complexity for the elliptical case. First, the change is not as remarkable as that on one-ring case. Secondly, it seems that narrower width of AOA does not bring the improvement of the BER performance.

References

1. Aissa, S., Aniba, G.: BER Analysis of M-QAM with Packet Combining over Space-time Block Coded MIMO Fading Channels. IEEE Transactions on Wireless Communications 7(3), 799–805 (2008)
2. Ahn, K.S., Heath, R.W., Baik, H.K.: Shannon Capacity and Symbol Error Rate of Space-time Block Codes in MIMO Rayleigh Channels with Channel Estimation Error. IEEE Transactions on Wireless Communications 7(1), 324–333 (2008)
3. Yue, S., Xiang-Gen, X.: Space-time Block Codes Achieving Full Diversity with Linear Receivers. IEEE Transactions on Information Theory 54(10), 4528–4547 (2008)
4. Maaref, A., Aissa, S.: Capacity of Space-time Block Codes in MIMO Rayleigh Fading Channels with Adaptive Transmission and Estimation Errors. IEEE Trans. On Wireless Com. 4(5), 2568–2578 (2005)
5. Gozali, R., Woerner, B.D.: On the Robustness of Space-time Block Codes to Spatial Correlation. In: Proc. IEEE Vehicular Technology Conf. (VTC-S 2002), Birmingham, Al, pp. 832–836 (2002)
6. Femenias, G.: BER Performance of Linear STBC from Orthogonal Designs over MIMO Correlated Nakagami-m Fading Channels. IEEE Transactions on Vehicular Technology 53, 307–317 (2004)
7. Il-Min, K.: Exact BER Analysis of OSTBCs in Spatially Correlated MIMO Channels. IEEE Trans. On Wireless Com. 54(8), 1365–1373 (2006)
8. Yu, K., Ottersten, B.: Models for MIMO Propagation Channels: A Review. Wireless Communications and Mobile Computing, Special Issue on Adaptive Antennas and MIMO Systems 2(7), 653–666 (2002)
9. Pätzold, M., Hogstad, B.O., Youssef, N.: Modeling, Analysis, and Simulation of MIMO Mobile-to-mobile Fading Channels. IEEE Transactions on Wireless Communications 7(2), 510–520 (2008)
10. Rafiq, G., Kontorovich, V., Pätzold, M.: On the Statistical Properties of the Capacity of Spatially Correlated Nakagami-M MIMO Channels. In: IEEE Vehicular Technology Conference VTC Spring 2008, pp. 500–506 (2008)
11. Luo, J., Zeidler, J.R., McLaughlin, S.: Performance Analysis of Compact Antenna Arrays with MRC in Correlated Nakagami-fading Channels. IEEE Trans. Veh. Technol. 50, 267–277 (2001)
12. Abdi, A., Kaveh, M.: A space C time Correlation Model for Multielement Antenna Systems in Mobile Fading Channels. IEEE J. Select. Areas Commun. 20, 550–560 (2002)

13. James, A.T.: Distributions of Matrix Variate and Latent Roots Derived from Normal Samples. Ann. Math. Statist. 35, 475–501 (1964)
14. Hogstad, B.O., Pätzold, M., Chopra, A.: A Study on the Capacity of Narrow and Wideband MIMO Channel Models. In: Proc. 15th IST Mobile & Communications Summit, IST 2006, Myconos, Greece (2006)
15. Leila, M., Mischa, D., Reza Nakhai, M., Aghvami, A.H.: Closed-form Capacity Expressions of Orthogonalized Correlated MIMO Channels. IEEE Commun. Lett. 8(6), 365–367 (2004)